TOWARD VALIDATION OF SIMULATED ACCELEROGRAMS VIA PREDICTION EQUATIONS FOR NONLINEAR SDOF RESPONSE

F. De Luca[1†], G. Ameri[2], I. Iervolino[1], F. Pacor[2], D. Bindi[3]

[1]*Dipartimento di Ingegneria Strutturale, Università degli Studi di Napoli Federico II, Via Claudio, 21 80125, Naples, Italy.*

[2]*Istituto Nazionale di Geofisica e Vulcanologia, Via Bassini 15, 20133, Milan, Italy.*

[3]*Deutsches GeoForschungsZentrum GFZ, Centre for Disaster Managment (CEDIM), Telegrafenberg, 14473 Potsdam, Germany.*

ABSTRACT

Seismic structural risk analysis of critical facilities may require nonlinear dynamic analysis for which record selection is one of the key issues. Notwithstanding the increasing availability of database of strong-motion records, it may be hard to find accelerograms that fit a specific scenario (e.g., in terms of magnitude and distance) resulting from hazard assessment at the site of interest. A possible, alternative, approach can be the use of artificial and/or simulated ground motion in lieu of real records. Their employment requires systematic engineering validation in terms of structural response and/or seismic risk. Prediction equations for peak and cyclic inelastic single degree of freedom systems' response, based on Italian accelerometric data, are discussed in this study as a possible benchmark, alongside real record counterparts, for the validation of synthetic records. Even if multiple events would be in principle required, an extremely preliminary validation is carried out considering only four simulated records of the 1980 Irpinia (Southern Italy) M_w 6.9 earthquake. Simulated records are obtained through a broadband hybrid integral-composite technique. Results show how this simulation method may lead to generally acceptable results. It is also emphasized how this kind of validation may provide additional results with respect to classical signal-to-signal comparison of real and simulated records.

1. INTRODUCTION

Modern earthquake design and assessment procedures are based on the evaluation of inelastic deformations of structures. In this framework, nonlinear structural analysis methods have earned increasing interest in scientific and professional communities. In particular, nonlinear dynamic analysis is becoming more common, especially for the design and the assessment of critical facilities (De Luca et al. 2011). On the other hand, nonlinear dynamic analyses require proper input selection. Thus, ground motion selection methods improved significantly in accuracy (PEER 2009). Notwithstanding the increased availability of strong-motion databases, it may be difficult to find real records' sets that fit specific scenarios (e.g., large magnitude, small source-to-site distance). An attractive approach can be to provide alternative seismic input, such as *artificial* or *simulated* records. However, the employment of these kinds of records in structural analysis requires systematic validation (e.g., Bazzurro and Luco 2004; Iervolino et al. 2010). It is important to assess whether recorded motions can be substituted by those artificial or simulated, and in which situation such replacement can be acceptable in terms of structural response.

The main target of engineering validation of *alternative* accelerograms should be to check whether these lead to the same seismic risk, that is the probability of failure, or loss estimation, with respect to nominally equivalent real records, when employed in performance-based

† flavia.deluca@unina.it

earthquake engineering (PBEE); i.e., Cornell and Krawinkler 2000, Krawinkler and Miranda 2004. This approach represents a complementary perspective with respect to the direct, and more common, comparison of real waveforms with their simulated counterpart.

Intermediate validation steps (between visual record comparison and full risk assessment) are real-to-simulated comparisons in terms of peak and cyclic nonlinear structural response of single degree of freedom (SDOF) systems (Iervolino et al. 2010, Galasso et al. 2012).

The objective of this work is to present a first step toward a comprehensive validation of simulated records through comparison between structural responses of synthetic records and empirical ground motion prediction equations (GMPEs), calibrated on real accelerograms. This approach considers both peak and cyclic inelastic responses taking as a benchmark the output of prediction equations. It is to note that all real-to-simulated comparisons (even if made in terms of nonlinear structural response) are pursuable only when a real records' benchmark is available, while validation through prediction equations, in principle, does not need the real records correspondent to the simulation. In turn, for this kind of comparison records from multiple events should be available.

The set of synthetic records, considered in this preliminary study, is calculated for four sites that recorded the 1980 (M_w 6.9) Irpinia earthquake (Ameri et al. 2011), with the broadband hybrid integral-composite (HIC) technique employing full-wavefield Green's function (Gallovič and Brokešová 2007); see section 2.

Prediction equations (De Luca 2011) in terms of peak and cyclic inelastic intensity measures, IMs, based on a constant strength reduction factor approach, are described in section 3. Peak inelastic displacement and equivalent number of cycles are the ground motion intensity measures selected. The prediction equations have been developed for several nonlinear SDOF systems, based on a large set of ground motion data from the ITalian ACcelerometric Archive or ITACA (Luzi at al. 2008; Pacor et al. 2011).

Results of the preliminary synthetic-to-GMPE comparison, made on the basis of the prediction equations, are provided in section 4. Finally, these results are also compared with that of a direct real-to-simulated comparison.

2. GROUND MOTION SIMULATION

The set of synthetic accelerograms adopted in this study is taken from Ameri et al. (2011). The authors, first modeled some ground motions recorded during the 1980 Irpinia earthquake in order to validate, from a seismological point of view, the generated synthetic seismograms. Then, several possible rupture processes of the Irpinia fault were considered, and the ground motion from these different "realizations" of the event, were calculated. This latter step was to capture the variability of the ground motion due to unknowns about the rupture. In particular, 54 different rupture processes were assumed for this fault, considering 6 possible positions of the hypocenter, 3 values of the velocity of the rupture propagation and 3 different distributions of the slip on the fault. The 54 rupture models are intended to capture the first-order uncertainties in the parameters or, in other words, the variability in the ground motion due to uncertainty in the source parameter assuming a limited number of alternative models. These kinematic rupture parameters were constrained to vary according to the ranges reported in Ameri et al. (2011) and were selected in order to sample scenarios that could happen during the actual earthquake. For instance, some of the rupture processes may generate large motions at some sites due to directivity effects, or particularly high rupture velocity or proximity to a slip asperity. These alternative models are considered equally probable having no justifiable reason to give more weight to one model with respect to another. All the rupture scenarios are characterized by the

same magnitude (M_w 6.9, the same as the 1980 earthquake) and the ground motion is simulated at different distances, according to the site locations. Thus, for each site a set of 54 synthetic accelerograms is available, with the same magnitude and distance values. Four sites (Table 1), located at different distances and positions around the fault, have been selected. Moreover, since local site effects are not included in the simulations, those sites were chosen because, according to Ameri et al. (2011), local amplification does not significantly affect the ground motion.

The adopted simulation methodology is here briefly described in order to stress that, differently from artificial or purely stochastic seismograms (e.g., Mucciarelli et al. 2004; Gasparini and Vanmarke 1976), the calculated synthetics are based on a more physical modeling of the earthquake source and wave propagation processes. The HIC technique simulates the rupture process in terms of slipping of elementary subsources with fractal number-size distribution (fractal dimension 2), randomly placed on the fault plane (Zeng et al. 1994). At low frequencies, the source description is based on the representation theorem (integral approach, Aki and Richards 2002), assuming a final slip distribution composed from the subsources, which is characterized by a *k-squared* decay (Herrero and Bernard 1994; Gallovič and Brokešová 2004). At high frequency, instead, the ground motion synthesis is obtained summing the contributions from each individual subsource treated as a point source (composite approach). The Green's functions for both frequency bands are evaluated by the discrete wavenumber technique (Bouchon 1981) in a layered 1D medium. This approach assures a broadband frequency content that satisfies the engineering needs. Moreover, as desirable, the model will produce coherent motion in the low-frequency band, generating for instance directivity pulses, and incoherent motion in the high-frequency one.

Table 1. Simulated records for the 1980 M_w 6.9 Irpinia earthquake (Ameri et al. 2011), name of the station (*Station*), code of the station (*Code*), epicentral distance (R_{epi}), Joyner and Boore distance (R_{JB}), soil class according to Eurocode 8 (*EC8 class*)

Station	Code	R_{epi} [km]	R_{JB} [km]	EC8 class
Bagnoli	BGI	22	7	B
Benevento	BNV	58	28	B
Bisaccia	BSC	28	18	A
Bovino	BVN	54	35	B

3. PREDICTION EQUATIONS FOR NONLINEAR SDOF RESPONSE

Inelastic displacement of SDOF systems employed as an IM for probabilistic seismic hazard analysis, or PSHA (e.g., McGuire 2004), is a recent enhancement of earthquake engineering research. Indeed, PSHA carried out in terms of inelastic IMs provides the seismic threat at a site by means of a parameter more informative for engineering purposes. In fact, referring to the PBEE framework, previous studies (Tothong and Luco 2007; PEER 2009; Tothong and Cornell 2007) showed that the inelastic displacement of SDOF systems is *efficient*, *sufficient* and *robust to scaling*, at least when seismic risk assessment of first mode dominated structures is of concern.

Non-linear SODF response IMs require *ad hoc* attenuation relationship for their employment in practical applications (e.g., Lawson 1996; Borzi and Elnashai 2000; Tothong and Cornell 2006; Bozorgnia et al. 2010a and 2010b). The semi-empirical models considered in this study (De Luca 2011), and considered in the following as a point of comparison for simulated records, were developed for SDOFs that have backbones characterized by bilinear hardening shape. Two SDOFs' hysteretic loops have been considered: one with and one without

stiffness' degradation; they are named EPH-p and EPH-k respectively, see Figure 1a.

Structural response measures include both cyclic (e.g., energy dissipation) and peak response (e.g., maximum inelastic deformation) quantities. Elastic periods of the SDOFs range in a broad interval sampled by 20 values, from 0.04s to 2s. Level of nonlinearity is accounted for by different strength reduction factors (R_μ) equal to 2, 4, 6, and 8. A constant strength reduction factor approach is adopted allowing every single record to show inelastic response. Thus, the value of the yield strength (F_y) at a given oscillation period T is a record-specific quantity and it is computed according to Equation 1, being m the mass of the SDOF (always equal to 1 kg_{mass}), and being $Sa_{el\text{-}record}(T)$ the ground motion elastic spectral acceleration at period T.

Two IMs were selected: the displacement-based parameter is the peak inelastic displacement (Sd_i), while the cyclic-response-related parameter is the equivalent number of cycles (N_e); see Equation 2. The latter is given by the cumulative hysteretic energy (E_H), evaluated as the sum of the areas of the hysteretic cycles, normalized with respect to the largest cycle. The latter evaluated as the area underneath the monotonic backbone curve from the yielding displacement (Δ_y) to the peak inelastic displacement ($A_{plastic}$), see Figure 1b. E_H is evaluated from the force-deformation envelope of the SDOF, discarding the force contribution due to damping, characterized by 5% of the critical damping ratio. *N_e represents the number of cycles at the maximum plastic displacement that the structure can develop in order to dissipate the total amount of E_H* (Manfredi 2001) plus 1, and it has some correlation with integral strong motion parameters. N_e is equal to 1 in the case of elastic response (Iervolino et al., 2010a); when yielding displacement is not attained in the SDOF. On the other hand, the constant R_μ approach excludes *a priori* this case.

$$F_y = \frac{F_{el}}{R_\mu} = \frac{Sa_{el-record}(T)\cdot m}{R_\mu} \tag{1}$$

$$N_e = \frac{E_H}{A_{plastic}} + 1 \tag{2}$$

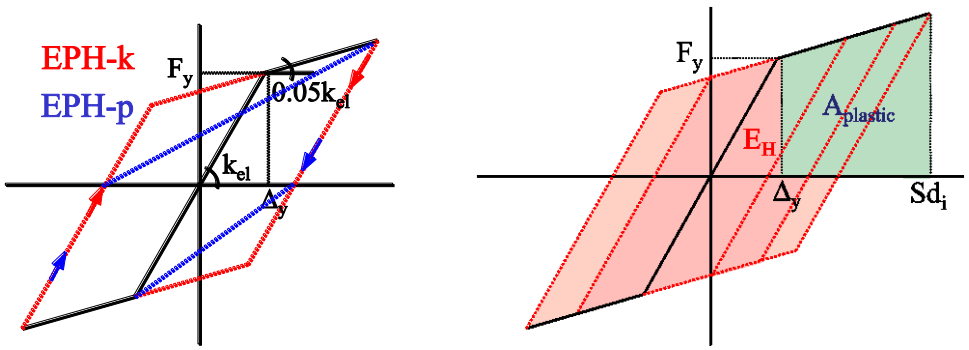

Figure 1. (a) EPH-k and EPH-p SDOF backbones; (b) definition of E_H and $A_{plastic}$ in the case of EPH-k SDOF backbone for the evaluation of N_e.

The dataset is comprised of 747 two-component waveforms from 103 earthquakes in the 4.1-6.9 M_w range, with hypocentral depth within 30 km, and recorded by 150 stations in the 0-200km distance range. The epicentral distance (R_{epi}), for magnitude lower than 5.5 events, and the closest distance to fault projection or Joyner and Boore distance (Joyner and Boore 1981), R_{JB},

for stronger earthquakes, were considered; see Figure 2. All stations are classified for site conditions following Eurocode 8 or EC8 (CEN 2004) categories. Five soil classes are considered: A, B, C, D, E. Most of site categories were assigned from geological and geophysical data (Di Capua et al. 2011), while about 30% from direct measurements of the value of the average shear wave velocity in the uppermost 30 meters, $V_{S,30}$.

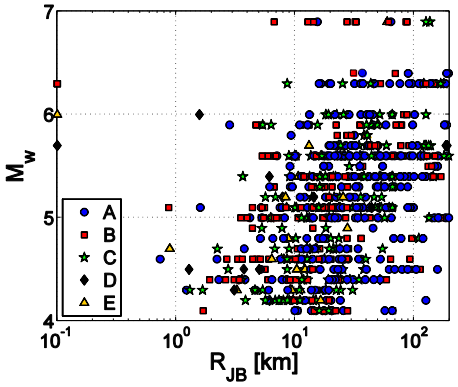

Figure 2. Dataset: magnitude versus distance (R_{epi} or R_{JB}) plot of the dataset, grouped according to the Eurocode 8 (CEN 2004) site classification.

To establish the functional form to predict the inelastic IMs, the model proposed by Bindi et al. (2011), for elastic spectral acceleration response spectra, was considered first. The prediction equation models have the general form of Equation 3, being Y the geometric mean of the North-South and East-West components for Sd_i or N_e. F_D, F_M, F_S, and F_{R_μ} are functions describing distance, magnitude, site amplification, and nonlinearity dependence of the IMs, while a is a constant term. The specific expressions to be adopted in the case of Sd_i are F_{D1} and F_{M1}; while in the case of N_e are F_{D2} and F_{M2}, as shown in Equation 4 to Equation 7. As mentioned, magnitude measure is M_w, distance is R_{JB}, or R_{epi} (in km). M_{ref}, M_h, R_{ref} are constants. The term F_S is given by $F_S=s_jC_j$, for $j=1,\ldots,5$, where s_j are the coefficients, while C_j are dummy variables used to denote the five different EC8 site classes (A to E). The term F_{R_μ} is given by $F_{R_\mu}=r_kC_k$, for $k=2,4,6,8$, where r_k are the coefficients, and C_k are dummy variables used to denote the four different strength reduction factors considered. In the regressions, s_1 (corresponding to EC8-A site class) and r_2 (corresponding to R_μ=2) were constrained to be equal to 0.

As a side result, and employing the same functional form of Equation 3 to Equation 5, obviously excluding the F_{R_μ} term, also a prediction equation for elastic displacements ($Sd_{elastic}$) was obtained. Regression coefficients for elastic, inelastic displacements, and equivalent number of cycles for EPH-k and EPH-p systems, not reported here for the sake of brevity, can be found in (De Luca 2011).

An example of the performance of the predictive models is shown Figure 3, where the estimates for a magnitude 6.0 earthquake at two periods (T equal to 0.2s and 1.0s) are plotted as a function of distance for the A site class and R_μ=4. The predictions are reported for both the considered systems (EPH-k and EPH-p) and they are compared with Sd_i or N_e data for a magnitude interval of 6.0±0.3. As expected, the differences in the hysteretic loop between EPH-k and EPH-p systems have an effect on cyclic response, while peak estimates are similar in the two cases.

The standard deviation of residuals (σ_{logY}) associated to the median of the predictions equations are shown in Table 2 for $Sd_{elastic}$, Sd_i, and N_e for both the EPH-k and EPH-p SDOF

systems. For each IM considered, the total (σ_{TOT}), the between-event (σ_B), or inter-event, and within-event (σ_W), or intra-event, standard deviations are shown as well. The values of σ_B and σ_W presented in this study were not published in De Luca (2011) where only σ_{TOT} was given.

The within-event variability (σ_W) is generally larger than the between-event (σ_B) standard deviation, for elastic and inelastic spectral displacements, for both the SDOFs considered, and it becomes prominent in the case of equivalent number of cycles. N_e is characterized by smaller σ_{TOT}, σ_B, and σ_W with respect to Sd_i. This trend may be a result of the integral and normalized nature of this IM.

$$\log_{10}(Y) = a + F_D + F_M + F_S + F_{R_\mu} \tag{3}$$

$$F_{D1} = \left[c_1 + c_2\left(M - M_{ref}\right)\right]\log_{10}\left(\sqrt{R_{JB}^2 + h^2}\,/\,R_{ref}\right) \tag{4}$$

$$F_{M1} = \begin{cases} b_1\left(M - M_h\right) + b_2\left(M - M_h\right)^2 & for\ M \le M_h \\ b_3\left(M - M_h\right) & otherwise \end{cases} \tag{5}$$

$$F_{D2} = c_1 \cdot \log_{10}\left(\sqrt{R_{JB}^2 + h^2}\,/\,R_{ref}\right) \tag{6}$$

$$F_{M2} = \begin{cases} b_1\left(M - M_h\right) & for\ M \le M_h \\ b_3\left(M - M_h\right) & otherwise \end{cases} \tag{7}$$

Table 2. Standard deviation of residuals (σ_{logY}) associated to the median prediction on the models in Equation 2.

T[s]	$Sd_{elastic}$			$Sd_{i,EPH-k}$			$Sd_{i,EPH-D}$			$N_{e,EPH-k}$			$N_{e,EPH-D}$		
	σ_{TOT}	σ_B	σ_W	σ_{TOT}	σ_B	σ_W	σ_{TOT}	σ_B	σ_W	σ_{TOT}	σ_B	σ_W	σ_{TOT}	σ_B	σ_W
0.04	0.361	0.222	0.285	0.400	0.281	0.284	0.381	0.270	0.269	0.184	0.108	0.148	0.191	0.116	0.152
0.07	0.371	0.218	0.299	0.401	0.278	0.288	0.388	0.274	0.276	0.177	0.101	0.146	0.193	0.108	0.160
0.1	0.379	0.227	0.304	0.391	0.268	0.284	0.385	0.270	0.274	0.169	0.092	0.142	0.186	0.104	0.154
0.15	0.384	0.247	0.293	0.381	0.259	0.280	0.378	0.262	0.273	0.159	0.085	0.134	0.172	0.096	0.142
0.2	0.401	0.275	0.291	0.376	0.257	0.274	0.378	0.260	0.274	0.150	0.077	0.128	0.162	0.090	0.135
0.25	0.395	0.274	0.285	0.377	0.256	0.276	0.379	0.262	0.274	0.152	0.077	0.131	0.163	0.093	0.134
0.3	0.380	0.271	0.266	0.377	0.259	0.274	0.383	0.266	0.275	0.150	0.077	0.128	0.162	0.093	0.132
0.35	0.369	0.262	0.259	0.375	0.260	0.270	0.380	0.265	0.273	0.153	0.082	0.130	0.161	0.092	0.132
0.4	0.357	0.251	0.253	0.372	0.260	0.266	0.378	0.264	0.271	0.150	0.079	0.128	0.159	0.091	0.130
0.45	0.355	0.244	0.258	0.373	0.261	0.266	0.379	0.264	0.272	0.154	0.083	0.130	0.160	0.092	0.131
0.5	0.352	0.238	0.258	0.373	0.263	0.265	0.380	0.265	0.271	0.154	0.081	0.130	0.158	0.092	0.129
0.6	0.358	0.249	0.257	0.373	0.265	0.263	0.380	0.267	0.270	0.153	0.083	0.128	0.158	0.092	0.128
0.7	0.358	0.247	0.258	0.372	0.265	0.261	0.382	0.270	0.270	0.154	0.082	0.130	0.159	0.094	0.128
0.8	0.360	0.250	0.259	0.373	0.265	0.263	0.382	0.268	0.272	0.154	0.081	0.131	0.156	0.089	0.128
0.9	0.364	0.252	0.263	0.375	0.267	0.264	0.384	0.271	0.272	0.151	0.076	0.130	0.150	0.083	0.125
1	0.365	0.255	0.261	0.378	0.269	0.265	0.384	0.271	0.272	0.148	0.078	0.126	0.149	0.084	0.123
1.25	0.371	0.255	0.270	0.382	0.275	0.266	0.388	0.273	0.275	0.148	0.080	0.125	0.146	0.086	0.118
1.5	0.380	0.257	0.280	0.386	0.272	0.273	0.389	0.271	0.280	0.153	0.081	0.129	0.146	0.085	0.119
1.75	0.384	0.256	0.285	0.386	0.270	0.276	0.391	0.272	0.281	0.158	0.072	0.141	0.146	0.082	0.121
2	0.378	0.245	0.287	0.388	0.271	0.278	0.392	0.271	0.283	0.171	0.076	0.153	0.151	0.086	0.124

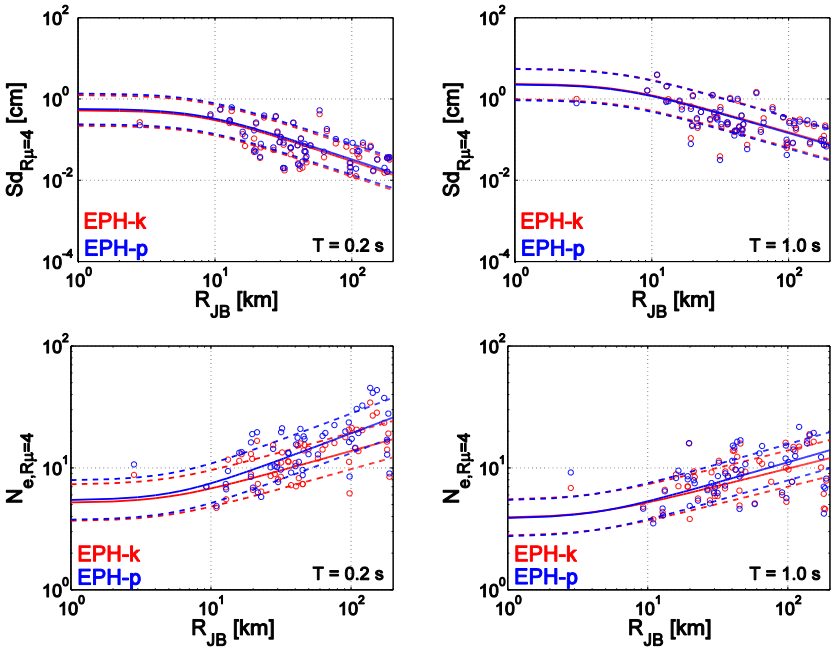

Figure 3. Sd_i and N_e estimates for a magnitude 6.0 earthquake, soil type A and R_μ equal to 4 at two natural periods (T = 0.2s and 1.0s) for both EPH-k and EPH-p systems, plotted as a function of R_{JB} and compared with the corresponding data for a magnitude interval of 6.0 ± 0.3.

4. ANALYSES AND RESULTS

The preliminary validation carried out herein is provided for the simulated records at four sites for the 1980 (M_w 6.9) Irpinia earthquake, described in section 2, and employing as benchmark the prediction equations described in section 3.

Table 1 shows stations' identifiers, distances and EC8 soil classification of the sites. Figure 4 shows the first comparison in terms of $Sd_{elastic}$. In Figure 4, elastic displacement spectra are plotted for both the 54 simulated seismograms (grey solid lines), their median, and the real records; then, they are compared with the median estimates of the GMPE (black solid lines). The standard deviation bands are computed as $10^{m_{\log Y} \pm \sigma}$, in which m_{logY} is the median estimate of the GMPE and σ is the standard deviation of the logarithm.

Two different σ have been employed: the total standard deviation (σ_{TOT}), and the within or intra-event standard deviation (σ_W), represented in Figure 4 with dotted lines. The 54 simulations depict a significant variability of the elastic spectral ordinates that is produced by the variations of the kinematic rupture parameters. It is worth noting that such variability is, in any case, of the same order of the $\pm\sigma_W$ bands associated to the median empirical estimations. In the following, when referring to over- or under- estimation, it is meant that the simulated records are lower or higher than the median estimate, and they are outside the $\pm\sigma$ bands evaluated as described above.

For some periods and sites, some underestimation can be observed when comparing simulations with GMPE's estimates. However, this applies also to real records. In fact, the observed spectra are generally enclosed in simulated ones. Especially the results at BNV and BVN stations imply that the ground motion recorded from the Irpinia earthquake was *smaller*

than that predicted by a GMPE developed for the whole Italian territory[‡]. It is also important to stress that only BGI record is included in the dataset employed for the estimation of the prediction equations.

Figure 5 shows the same plots provided in Figure 4. In this case the comparisons are carried out in terms of Sd_i for EPH-k system, and R_μ=4 and R_μ=8. For BNV and BVN stations both simulated and real records are below the median from GMPE.

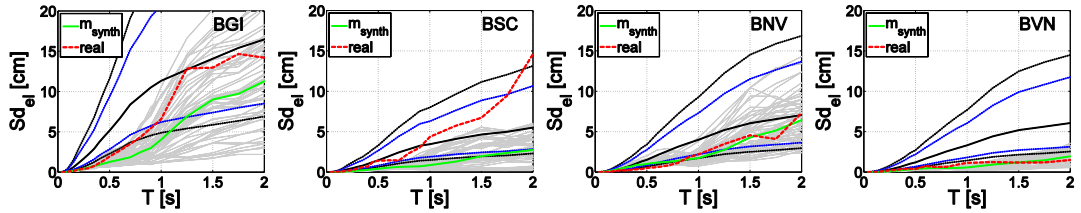

Figure 4. Median spectra of the prediction equation for $Sd_{elastic}$ with their $\pm\sigma_{TOT}$ and $\pm\sigma_W$ bands compared with the corresponding spectra of the 54 simulated, their median (m_{synth}), and the real (*real*) records at the stations BGI, BSC, BNV, and BVN.

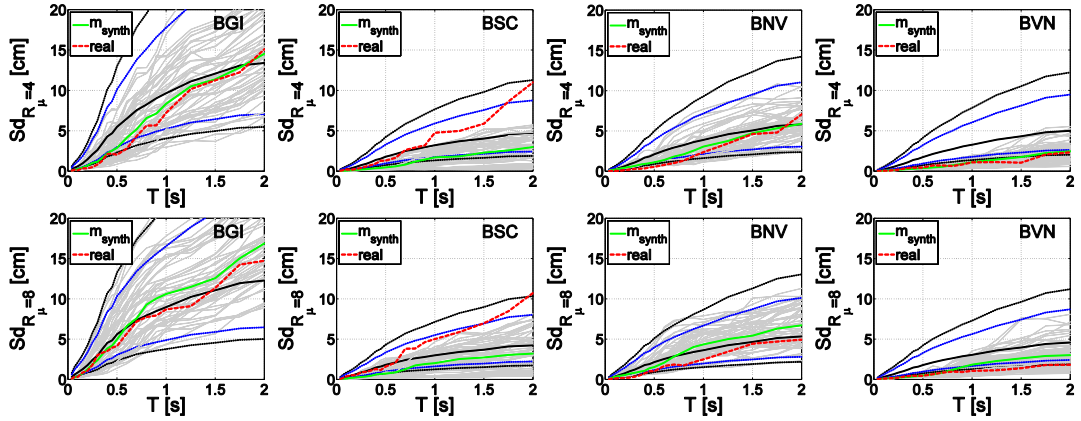

Figure 5. Median spectra of the prediction equation for Sd_i, EPH-k system, R_μ=4 and 8, with their $\pm\sigma_{TOT}$ and $\pm\sigma_W$ bands compared with the corresponding spectra of the 54 simulated, their median (m_{synth}), and the real (*real*) records at the stations BGI, BSC, BNV, and BVN.

The very preliminary comparison with the prediction equations in terms of peak elastic and inelastic response suggests that the simulated records generated with HIC technique may be considered compatible with what expected from real records. Such results may find some analogy with the findings regarding peak inelastic response of artificial records, (different in nature with respect to those synthetic herein), when compared to real records in the case of response spectrum matching criterion (Iervolino et al. 2010).

In Figure 6 and Figure 7, N_e spectra are shown in the case of R_μ=4 and R_μ=8, for both EPH-k and EPH-p SDOFs, respectively. In the case of N_e response (representative of cyclic response), both EPH-k and EPH-p SDOF have been considered; given the differences observed in the trends shown in Figure 3. For both EPH-k and EPH-p, the 54 simulations provide a cyclic

[‡] In this sense, it is to note that the bias of the mean of data from the Irpinia earthquake was not removed when making the comparison.

response generally around or below the $-\sigma$ band of the GMPE; i.e., systematically lower than the median estimate of the GMPE. However, again, also the real counterparts of the simulation are mostly below the median from the GMPE.

In Figure 6 and 7, it is also confirmed the typical trend of N_e spectra. In fact, they are characterized by a strictly decreasing trend: high values for small period range, and a more mild decay in the medium-to-long period range (see Manfredi 2001; Iervolino et al. 2010).

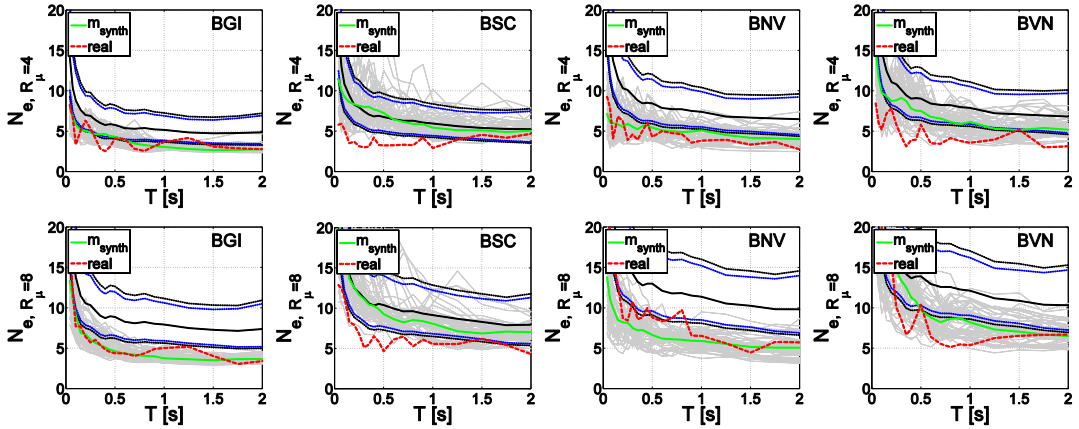

Figure 6. Median spectra of the prediction equation for N_e, EPH-k system, R_μ=4 and 8, with their $\pm\sigma_{TOT}$ and $\pm\sigma_W$ bands compared with the corresponding spectra of the 54 simulated, their median (m_{synth}), and the real (*real*) records at the stations BGI, BSC, BNV, and BVN.

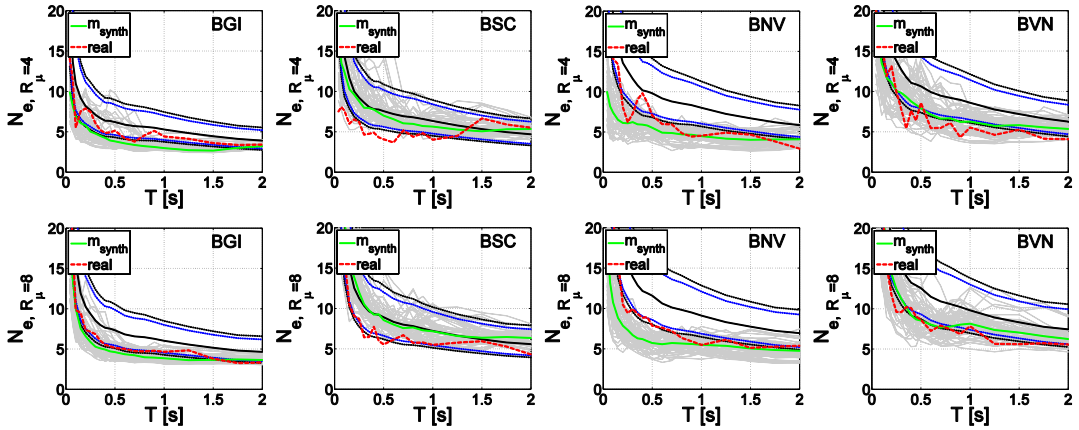

Figure 7. Median spectra of the prediction equation for N_e, EPH-p system, R_μ=4 and 8, with their $\pm\sigma_{TOT}$ and $\pm\sigma_W$ bands compared with the corresponding spectra of the 54 simulated, their median (m_{synth}), and the real (*real*) records at the stations BGI, BSC, BNV, and BVN.

The slight underestimation of N_e spectra in simulated records, at some stations, may also have a reason in the fact that the HIC synthetic records in the study use a 1D crustal model. Indeed, the complexity of the Earth's crust produces a number of reflected and refracted waves that increase the overall duration of the seismogram with respect to a simple 1D model.

The above preliminary findings on cyclic response of simulated records are significantly different with respect to the findings for cyclic response to spectral matched artificial

accelerograms (Iervolino et al. 2010). In fact, artificial accelerograms are characterized by significant overestimation of the cyclic structural response. This difference may be expected because, artificial records does not explicitly account for source and path effect on durations, while they are intentionally designed to capture (elastic) spectral response.

In Figure 8, a comparison of the relative errors of the medians of the 54 simulations with respect to the median estimate of the GMPE (m_{synth} *vs* m_{GMPE}) and with respect to the real records (m_{synth} *vs real*) is carried out for the case of elastic displacements and peak and cyclic inelastic responses, for R_μ equal to 4. The expression for the evaluation of the relative errors in Figure 8 is shown in Equation 8. The symbol m_{synth} *vs* m_{GMPE}, in Figure 8, indicates the relative errors of the median value of the 54 simulations (m_{synth}) with respect to the median estimate of the GMPE (m_{GMPE}). The symbol m_{synth} *vs real*, in Figure 8, indicates the relative errors of m_{synth} with respect to the responses of the real records considered ($real_{spectral\text{-}response}$).

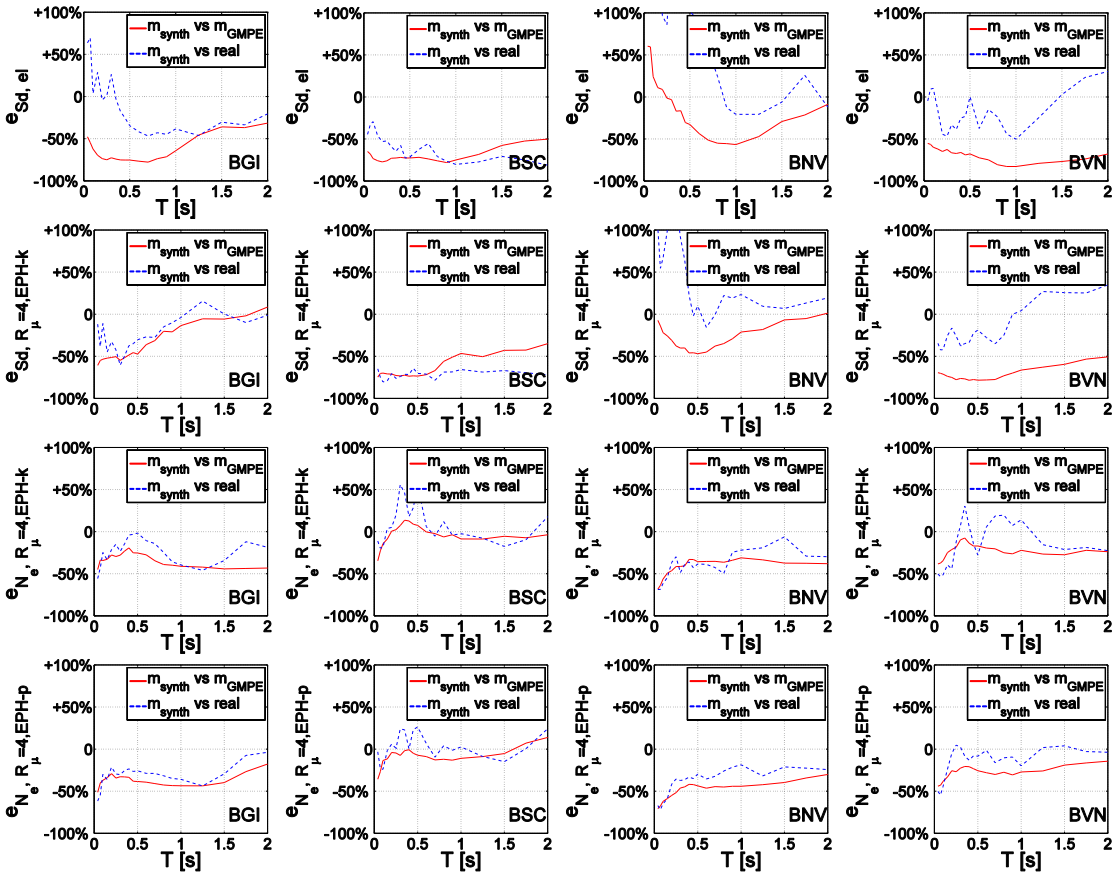

Figure 8. Relative errors of the median of the 54 synthetic records (m_{synth}) with respect to the median estimate of the prediction equation (m_{synth} *vs* m_{GMPE}) and with respect to real records (m_{synth} *vs real*) evaluated for $Sd_{elastic}$, Sd_i for the EPH-k system and N_e for both EPH-k and EPH-p systems for R_μ=4.

$$e_{m_{synth}\ vs\ GMPE} = \frac{m_{synth} - m_{GMPE}}{m_{GMPE}}; \quad e_{m_{synth}\ vs\ real} = \frac{m_{synth} - real_{spectral-response}}{real_{spectral-response}} \tag{8}$$

The comparisons in Figure 8 better quantify the results presented and discussed above. The average value of the relative errors of the simulations with respect to the GMPE (m_{synth} *vs GMPE*) can reach also 50% for both peak and cyclic response; however, at least some of this bias may be attributed to the fact that also real records generally show some bias with respect to the median from the GMPE.

4. CONCLUSIONS

Prediction equations in term of peak and cyclic inelastic response can be employed as a benchmark for engineering validation of simulated records. The validation made in terms of prediction equations, along with real records, lies at the core of the problem; in fact, as long as simulated records are employed in nonlinear dynamic analyses as substitutes of real records, the main target is that they lead to the same conclusion in terms of risk assessment.

An extremely preliminary (because using records from one event only) validation example, referred to the case of four sites for the 1980 Irpinia, M_w 6.9, earthquake was carried out focusing on the comparison of validation made by means of prediction equations along with the more typical simulated-to-real validation approach. In the example provided, *elastic displacements*, *inelastic displacements*, and *equivalent number of cycles*, for different strength reduction factors, were controlled as informative intensity measures for peak and cyclic response to be employed in the validation. The first, expected, conclusion is that nonlinear response rather than the only elastic one can provide additional significant results to the validation procedure.

The application carried out in the study found some agreement of the simulated records with respect to those real and general compatibility of the former with respect to the prediction equations in terms of non-linear SDOF response, also considering the used simulation model with respect to the actual 3-dimensional crustal structure.

Notwithstanding the very preliminary character of the results provided, given the small sample of records considered; the validation approach through prediction equations of peak and cyclic inelastic response is a first step towards a systematical engineering validation of physics-based simulated records.

ACKNOWLEDGMENTS

The study presented in this paper have been developed within the activities of the *Rete dei Laboratori Universitari di Ingegneria Sismica – ReLUIS* for the research program funded by the *Dipartimento della Protezione Civile* (2010-2013).

REFERENCES

Aki, K., and P. G. Richards, 2002. Quantitative Seismology, Second Ed. University Science Books, Sausalito, California, 704 pp.

Ameri G., Emolo A., Pacor F., Gallovic F., 2011. Ground motion simulations for the 1980 M 6.9 Irpinia earthquake (southern Italy) and scenario events. Bulletin Seismological Society of America, 101, 1136–1151.

Bazzurro P., Luco N., 2004. Post-elastic response of structures to synthetic ground motions. Report for Pacific Earthquake Engineering Research (PEER) Center Lifelines Program Project 1G00 Addenda. CA, US.

Bindi D., Pacor F., Luzi L., Puglia R., Massa M., Ameri G., Paolucci R., 2011. Ground motion prediction equations derived from the Italian strong motion database. Bulletin of Earthquake Engineering, 9, 1899-1920.

Borzi B., and Elnashai A.S., 2000. Refined force reduction factors for seismic design. Engineering Structures, 22, 1244–1260.

Bouchon, M., 1981. A simple method to calculate Green's functions for elastic layered media. Bulletin Seismological Society of America, 71, 959–971.

Bozorgnia Y., Hachem M.M., Campbell K.W., 2010a. Ground motion prediction equation ("attenuation relationship") for inelastic response spectra. Earthquake Spectra, 26, 1-23.

Bozorgnia Y., Hachem M.M., Campbell K.W., 2010b. Deterministic and probabilistic predictions of yield strength and inelastic displacement spectra. Earthquake Spectra, 26, 25-40.

Comité Européen de Normalisation (CEN), 2004. Eurocode 8 – Design of Structures for earthquake resistance – Part 1: General rules, seismic actions and rules for buildings. EN 1998-1, CEN, Brussels.

Cornell, C.A. and Krawinkler, H. , 2000. Progress and challenges in seismic performance assessment. PEER News, April 2000.

De Luca F., 2011. Records, capacity curve fits and reinforced concrete damage states within a performance based earthquake engineering framework. PhD thesis. Department of Structural Engineering, University of Naples Federico II. Advisors: G. Manfredi, I. Iervolino, G.M. Verderame. Available at http://wpage.unina.it/iuniervo/

De Luca F., Ameri G., Iervolino I., Pacor F., Bindi D., 2011. Prediction equations of nonlinear SDOF response: towards an enhancement of hazard analysis. 30° Convegno Nazionale GNGTS - Gruppo Nazionale di Geofisica della Terra Solida, 14-17 Novembre, 2011.

Di Capua G., Lanzo G., Pessina V., Peppoloni S., Scasserra G., 2011. The recording stations of the italian strong motion network: geological information and site classification. Bulletin of Earthquake Engineering, 9, 1779-1796.

Galasso C., Zareian F., Iervolino I., Graves R.W., 2012. Validation of ground motion simulations for historical events using SDOF systems. Bulletin of the Seismological Society of America, 102, 2727-2740.

Gallovič, F., and J. Brokešová, 2004. The k-2 rupture model parametric study: Example of the 1999 Athens earthquake. Studia Geophysica et Geodaetica, 48, 589–613.

Gallovič, F., and Brokešová J., 2007. Hybrid k-squared source model for strong ground motion simulations: Introduction. Physics of the Earth and Planetary Interiors, 160, 34–50.

Gasparini D.A., Vanmarke E.H., 1976. Simulated earthquake motions compatible with prescribed response spectra. MIT civil engineering research report R76-4. Massachusetts Institute of Technology, Cambridge, MA.

Herrero, A., and P. Bernard, 1994. A kinematic self-similar rupture process for earthquakes. Bulletin Seismological Society of America 84, 1216–1228.

Iervolino I., De Luca F., Cosenza E., 2010. Spectral shape-based assessment of SDOF nonlinear response to real, adjusted and artificial accelerograms. Engineering Structures, 32, 2776-2792.

Joyner W.B., Boore D.M., 1981. Peak horizontal acceleration and velocity from strong-motion records including records from the1979 Imperial Valley, California, earthquake. Bulletin of Seismological Society of America 71, 2011–2038.

Krawinkler H. and Miranda E., 2004. Performance-Based Earthquake Engneering. In: Bozorgnia Y. and Bertero V.V. Editors Earthquake Engineering: From engineering seismology to performance-based engineering, CRC Press, chapter 9.

Lawson, R. S., 1996. Site-dependent inelastic seismic demands. Ph.D. Thesis, Department of Civil Engineering, Stanford University, Stanford, CA.

Luzi L., Hailemikael S., Bindi D., Pacor F., Mele F., Sabetta F., 2008. ITACA (ITalian ACelerometric Archieve): A web portal for the dissemination of Italian strong-motion data, Seismological Research Letters, 79, 716-722.

Manfredi G., 2001. Evaluation of seismic energy demand. Earthquake Engineering and Structural Dynamics, 30(4), 485–499.

McGuire R.K., 2004. Seismic hazard and risk analysis. Report MNO-10. Earthquake Engineering Research Institute Publication, Oakland, CA, USA.

Mucciarelli M., Spinelli A., Pacor F., 2004. Un programma per la generazione di accelerogrammi sintetici "fisici" adeguati alla nuova normativa. XI Convegno ANIDIS, "L'Ingegneria Sismica in Italia". January 25-29, Genoa, Italy.

Pacor F, Paolucci R, Ameri G, Massa M, Puglia R, 2011. Italian strong motion records in ITACA: overview and record processing. Bulletin of Earthquake Engineering, 9, 1741.1759.

PEER ground motion selection and modification working group – Haselton C.B., editor, 2009. Evaluation of Ground Motion selection methods: prediction median interstory drift response of buildings. PEER report 2009/01.

Tothong P., Cornell C.A., 2006. An empirical ground motion attenuation relation for inelastic spectral displacement. Bulletin of the Seismological Society of America, 96, 2146-2164.

Tothong P., Cornell C.A., 2007. Probabilistic seismic demand analysis using advanced ground motion intensity measures, attenuation relationships, and near fault effects. John A. Blume Earthquake Engineering Center, Department of Civil and Environmental Engineering, Stanford University, CA 2007.

Tothong P., Luco N., 2007. Probabilistic seismic demand analysis using advanced ground motion intensity measures. Earthquake Engineering and Structural Dynamics, 36, 1837-1860.

Zeng, Y., J. G. Anderson, and G. Yu, 1994. A composite source model for computing realistic synthetic strong ground motions. Geophysical Research Letters. 21, 725–728.